Hybrid semiconductor nanowire-metallic Yagi-Uda antennas

Mohammad Ramezani,[†,‡] Alberto Casadei,[†] Grzegorz Grzela,[‡] Federico Matteini,[†] Gözde Tütüncüoglu,[†] Daniel Rüffer,[†] Anna Fontcuberta i Morral,[*,†] and Jaime Gómez Rivas[*,‡,¶]

Laboratoire des Matériaux Semiconducteurs,École Polytechnique Fédérale de Lausanne, 1015 Lausanne, Switzerland, Center for Nanophotonics, FOM Institute AMOLF, c/o Philips Research Laboratories, High Tech Campus 4, 5656 AE Eindhoven, The Netherlands, and COBRA Research Institute, Eindhoven University of Technology, P.O. Box 513, 5600 MB Eindhoven, The Netherlands

E-mail: anna.fontcuberta-morral@epfl.ch; rivas@amolf.nl

Abstract

We demonstrate the directional emission of individual GaAs nanowires by coupling this emission to Yagi-Uda optical antennas. In particular, we have replaced the resonant metallic feed element of the nanoantenna by an individual nanowire and measured with the microscope the photoluminescence of the hybrid structure as a function of the emission angle by imaging the back focal plane of the objective. The precise tuning of the dimensions of the metallic elements of the nanoantenna leads to a strong variation of the directionality of the emission, being able to change this emission from backward

[*]To whom correspondence should be addressed
[†]École Polytechnique Fédérale de Lausanne
[‡]FOM Institute AMOLF
[¶]Eindhoven University of Technology

to forward. We explain the mechanism leading to this directional emission by FDTD simulations of the scattering efficiency of the antenna elements. These results cast the first step toward the realization of electrically driven optical Yagi-Uda antenna emitters based on semiconductors nanowires.

Keywords

Semiconductor nanowire, Yagi Uda optical antenna, directional emission, Fourier microscopy

Due to the unique optical properties of semiconductor nanowires they are an excellent platform for opto-electronic and photonic applications.[1–3] The possibility of controlling their composition, geometry and crystallographic morphology opens up a great freedom in designing different devices with desired properties.[4] In recent years, several studies have been realized on optically[5] and electrically[6] driven nanolasers, solar cells,[7–9] optical switches,[10] and single photon sources coupled to optical waveguides.[11,12] The photoluminescence properties of nanowires and the coupling of their emission to leaky and guided modes have been studied extensively.[13–17] In addition, the coupling of nanowires with plasmonic nanostructures modifies their optical properties.[18–20] In parallel, in the past decade, many efforts have been done to enhance the efficiency and modify the direction of the emission of quantum emitters including quantum dots and fluorescent molecules.[21–25] Yagi-Uda optical antennas are an example of a structure showing a pronounced directionality of the emission.[24,26–31] In this system, the emission of a single quantum emitter couples to the antenna feed element, which is a metallic nanorod acting as a half-wavelength dipole nanoantenna. The permittivity of noble metals, including Au, Ag and Al, and the size of the nanorods leads to plasmonic resonances in the visible range of the electromagnetic spectrum. These resonances modify the spontaneous emission rate of nearby emitters due to the change of the local density of optical states.[32] Subsequently, the scattering of the feed element emission with the antenna elements and the interference of this scattered radiation in the far-field leads to a strong directional emission. This emission can be controlled by the resonant response of the elements forming the Yagi-Uda antenna and their spacing.

In this letter, we demonstrate a hybrid semiconductor-metal Yagi-Uda antenna. This hybrid system is realized by replacing the resonant metallic feed element of the Yagi-Uda by a non-resonant semiconductor nanowire. As we show, the non-resonant emission from the nanowire is not a limitation for the strong directional emission of the Yagi-Uda antenna. The measurements have been performed on GaAs nanowires using a Fourier microscope i.e., a microscope that images the reciprocal space or the angular distribution of the emission.

To demonstrate the strong dependence of the emission with the antenna parameters, we have fabricated two devices with different dimensions to direct the emission in opposite directions. The mechanism leading to the directional emission is studied by means of the Finite-difference Time-Domain (FDTD) method and explained in terms of the scattering efficiencies of the antenna elements. The results of this letter can be exploited for the development of electronically driven optical Yagi-Uda antennas for directional single photon emission. The schematic representation of the nanowire-Yagi-Uda hybrid system is shown in Fig. 1 (a). The antenna is formed by a GaAs nanowire (red bar in Fig. 1 (a)) acting as feed element of the emission; three metal rods acting as directors, and a bigger metal rod on the opposite side of the nanowire acting as reflector. The role of the directors is to beam the emission of reflector-nanowire pair into smaller solid angles toward their side. This solid angle is determined by the number of directors. Hybrid Yagi-Uda antennas were fabricated by the procedure explained in detail in the methods section. SEM images of the two investigated antennas are shown in Figs. 1 (b) and (c). The main difference between the antennas are the length of the reflectors and the distance between the elements. Detailed information of the dimensions of the antennas is available in the methods section. We name these antennas as YU175 (Fig. 1 (b)) and YU300 (1 (c)) in reference to the length of their directors which is 175 nm and 300 nm, respectively. Note that the distance between the semiconductor nanowire and the metallic rods is relatively large (>100 nm). Therefore, we do not expect to have any strong modification of the luminescence decay rate in this system.[21,22,28]

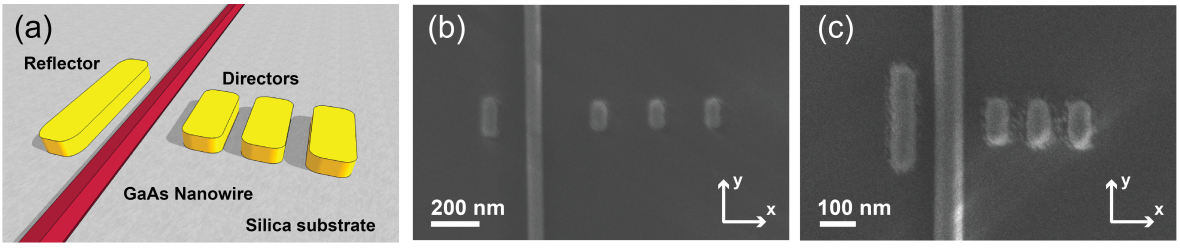

Figure 1: (a) Schematic representation of an hybrid nanowire-plasmonic Yagi-Uda antenna. The nanowire is represented by the long red structure, while the plasmonic reflector and directors are represented by the yellow rods. All structures are fabricated on silica substrates. (b) and (c) are SEM images of the hybrid nanowire-Yagi-Uda optical antennas. (b) Corresponds to YU175 with the reflector length of 175 nm and (c) to YU300 with the reflector length of 300 nm.

We have used Fourier microscopy to measure the directionality of the emission from the hybrid Yagi-Uda.[33] The schematic representation of the setup is shown in Fig. S1 (supplementary information). The nanowire is excited with a focused beam (FWHM $\simeq$ 650 nm) from a continuous wave laser diode (λ = 785 nm) by means of a 100$\times$ objective with a numerical aperture of 0.95. The illuminated power for all experiments is kept constant and equal to 25 mW. The photoluminescence is collected by the same objective and decomposed on the back focal plane of the objective in its plane wave components, each with a defined wave vector. This plane is imaged by the Fourier lens located at the distance $2f$, where f is its focal length. A charge-coupled device (CCD) camera is positioned at the distance $2f$ from the Fourier lens to obtain the image of the back focal plane of the objective. To detect only the emission of GaAs nanowires and to filter out the scattered light from the excitation laser, a band pass filter, 880$\pm$ 20 nm, followed by a notch filter at 785 nm were placed in front of the CCD camera.

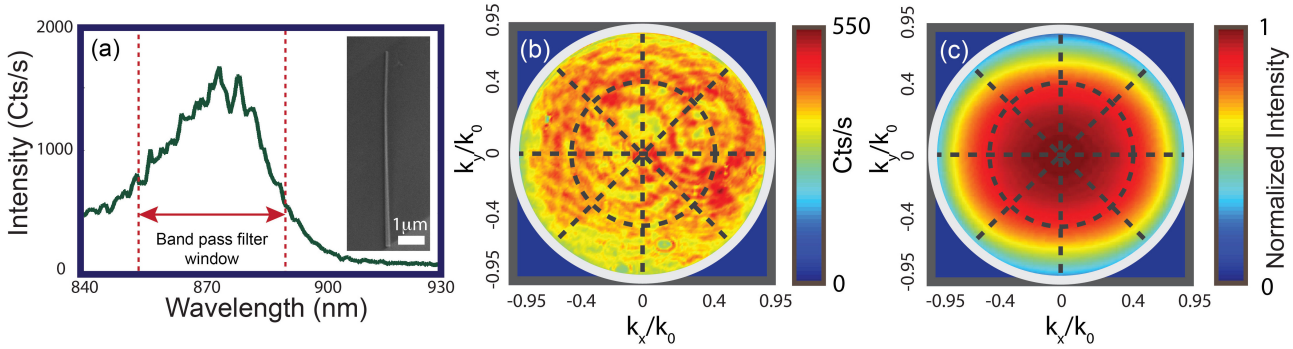

Figure 2: (a) Photoluminescence spectrum of a GaAs nanowire with diameter of 70 ± 5 nm. The SEM image of the nanowire on the silica substrate is shown in the inset of panel (a). The dotted lines indicate the band width of a filter used to collect only the nanowire emission in the Fourier measurements. (b) Radiation pattern of a GaAs nanowire in Fourier space. A relatively homogeneous emission across the Fourier plane can be seen. The light gray circle represents the collection angle of the objective with a numerical aperture of 0.95. (c) Simulation of the radiation pattern of a GaAs nanowire on a silica substrate. The simulated emission is normalized by its maximum value.

The photoluminescence spectrum of a bare GaAs nanowire at room temperature is shown in Fig. 2 (a). The peaked emission at $\lambda \sim 870$ nm is characteristic of GaAs nanowires. The SEM image of this nanowire is displayed in the inset of Fig. 2 (a). The Fourier emission pattern obtained from the bare nanowire is shown in Fig. 2 (b). The Fourier image represents the measurement of intensity in Cts/s in color scale as a function of the components of the emission wave vector in the plane of the sample (k_x, k_y) normalized by $k_0 = 2\pi/\lambda$. The light gray circle in the figure indicates the acceptance angle of the objective with a numerical aperture of 0.95. This emission exhibits centrosymmetric radiation pattern. The Finite-Difference Time-Domain (FDTD) simulation of the radiation pattern shown in Fig. 2 (c), and described in the method section, is in good agreement with the measurement.

To understand the physics leading to the radiation pattern shown in Fig. 2, We have calculated the dispersion of the guided and leaky modes supported by an infinitely long cylinder embedded in homogeneous medium[34] (See the Fig. S2 in the supplementary information). The fundamental mode (HE_{11}) is the only guided mode that is supported by GaAs nanowires with a diameter of 70 nm. However, the coupling efficiency of the nanowire emission to this

mode is low due to the mode profile extending mainly in the surrounding medium.[17] Therefore, most of the emission leaks out of the nanowire close the region where the nanowire is excited.[16] Hence, the far-field radiation pattern of the horizontal nanowire becomes highly non-directional as shown in Fig. 2 (b). This important characteristic facilitates the coupling of the emission from the nanowire to the metallic elements of the Yagi-Uda antenna.

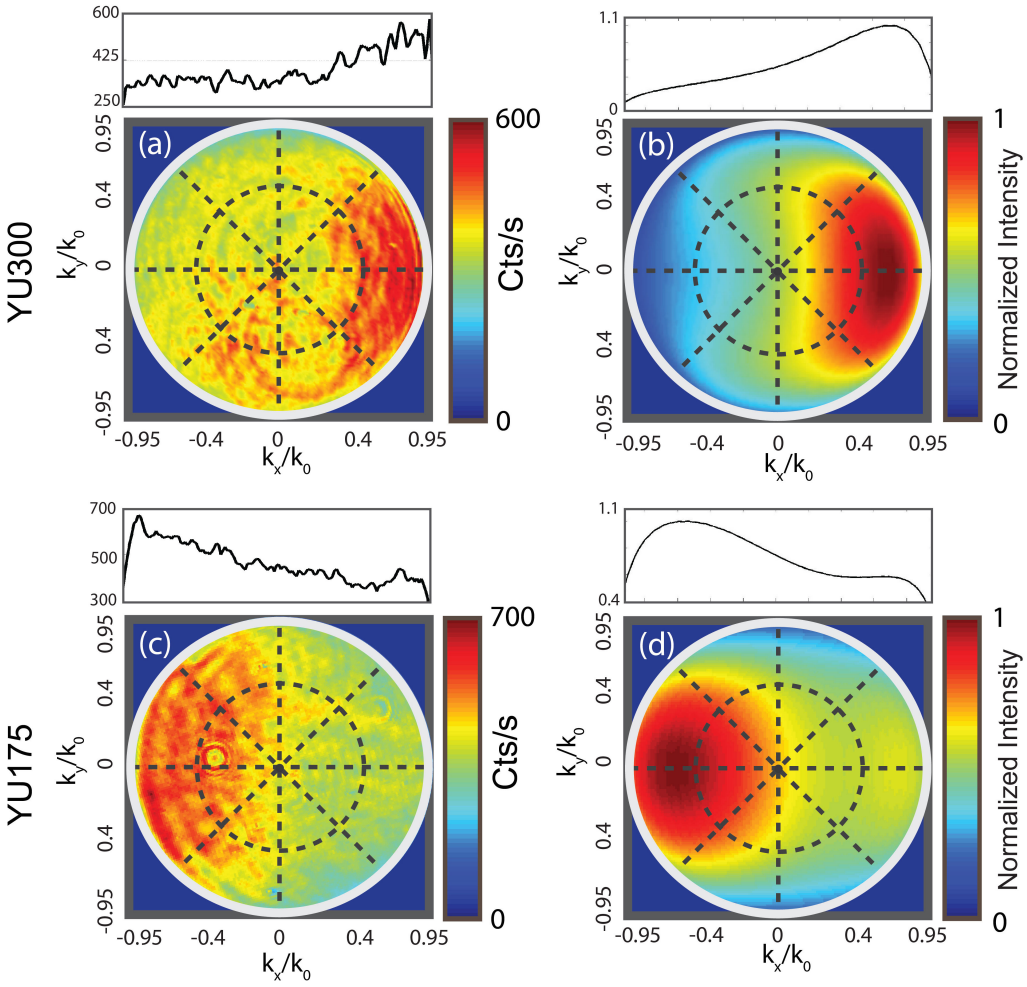

Figure 3: (a) Radiation pattern measurement of YU300. Most of the radiation is directed towards the reflector (right direction). (b) Simulation of the normalized radiation pattern of YU300. (c) Measurement of the radiation pattern from YU175. Most of the emission is directed towards the reflector (left direction). (d) Simulated radiation pattern of YU175 normalized by its maximum.

Figure 3 (a) shows the measurement of the radiation pattern of YU300. A large fraction of the radiation is directed toward the forward direction (the $k_x > 0$ direction), i.e., the directionality of the emission is toward the side of the directors of the Yagi-Uda antenna. Furthermore, a strong beaming that confines the emission in the range of $-0.4 < k_y/k_0 < 0.4$ can be seen. The FDTD simulation of the radiation pattern of this antenna is, shown in Fig. 3(b) and confirms the measurements with an excellent agreement. The effect of the reflector length on the directionality of the antenna emission is experimentally shown in Fig. 3 (c). By decreasing the length of the reflector element to 175 nm in YU175, the emission points toward the backward direction, i.e. the $k_x < 0$ direction. Moreover, a weaker directionality and beaming of the emission are obtained in this device.

One criterion in the assessment of the antenna performance is the Front to Back emission ratio (F/B). This factor is defined as the ratio between the emission intensity along the radiation direction defined by the directors ($k_x > 0$ in our antenna) and the intensity at the opposite direction. The F/B ratio for YU300 determined at $k_x/k_0 = 0.83$, i.e., the wave vector of maximum emission, is 1.8 for the experiment and 4 in the simulation. The difference between the experimental and theoretical F/B values can be attributed to the background intensity in the far-field radiation pattern originating from the excitation of the nanowire. As discussed on the methods section, to simulate the radiation pattern of the devices, a single electrical dipole is placed in the middle of the nanowire, oriented along its long axis.[35,36] Consequently, a very localized excitation of the emission is considered for the simulations. However, in experiments the nanowire is excited by a diffraction-limited focused laser spot. This illumination excites regions of the nanowire relatively far from the Yagi-Uda elements and introduces a background intensity in the directional emission pattern. Another source that can lead to the background emission is the excitons diffusion along the nanowire. Typical exciton diffusion length for these type of GaAs nanowires is $< 1\ \mu m$.[37] This is comparable with the size of the excitation beam. Therefore, it is not possible to distinguish from the measurements what the origin of the emission background is. However,

this background could be significantely reduced if embedded heterostructures or quantum dots are used as the emission source. For YU175, the F/B ratios defined at the same k_x/k_0 as for YU300 are 0.48 (experiment) and 0.62 (simulation). These F/B ratios smaller than 1 indicate beaming of the emission along the wrong direction. The response of YU175 is thus dominated by the large scattering efficiency of the reflector, resulting for its resonant behavior at the nanowire emission wavelength, and the directors do not have a significant influence on the emission directionality.

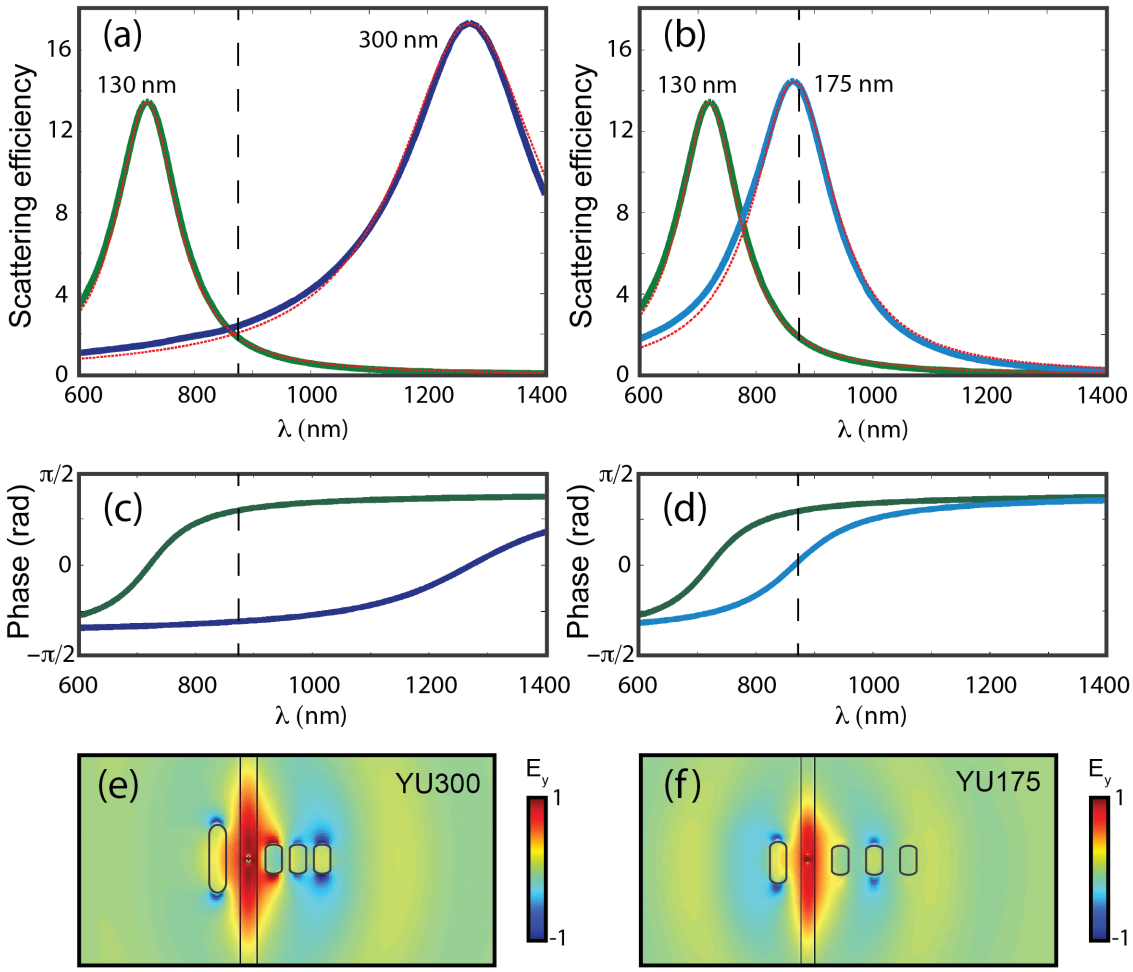

Figure 4: Numerical simulations of the scattering efficiency of Au rods with a height of 50 nm and a width of 60 nm on a silica substrate. (a) Simulation of two rods with lengths of 130 and 300 nm representing the directors and reflector of YU300. (b) as in (a) but for rods with a length of 130 and 175 nm representing the directors and reflector of YU175. The emission peak of the GaAs nanowire (λ = 870 nm) is indicated by the black dashed line in both panels. The red dotted curves are Lorentzian fits to the scattering efficiency simulations. (c) and (d) are the calculated phase of the Lorentzian oscillators in panels (a) and (b), respectively. (e) and (f) Snapshots from the FDTD simulation of the normalized amplitude of the y-component of the electric near-field in YU175 and YU300, respectively.

In order to give a simple description in the mechanism leading to the pronouncedly different directionality of the emission of different antennas, we have numerically calculated the scattering efficiency of Au rods with the dimensions of the antenna elements, i.e., width of 60 nm, height of 50 nm and with different lengths, placed on a silica substrate. The length of the rod is varied between 130 nm to 300 nm. The scattering efficiency is defined as the

scattering cross section normalized by the geometrical cross section of the rod. The metallic rod is illuminated at normal incidence by a polarized plane wave along the length of the rod. The calculated values of the scattering efficiency are shown in Figs. 4 (a) and (b) for the director and reflector rods of YU300 and YU175, respectively. The corresponding absorption efficiencies are given in Fig. S3 in the supplementary information. These absorption efficiencies are $\simeq 5$ times lower than the scattering efficiencies. Therefore, the dominant mechanism leading to the directional emission can be ascribed to scattering. The scattering efficiency exhibits the characteristic resonant behavior due to a localized surface plasmon polariton, i.e., the coherent oscillation of the free electrons in the metallic rod. These resonances correspond to the lowest order plasmonic mode, i.e., the $\lambda/2$ resonance. As expected, a considerable red-shift of the resonance frequency occurs by increasing the length of the rod. The scattering efficiency of each rod can be considered as a reliable criteria for selecting the proper geometrical parameters to control the directional emission of a Yagi-Uda antenna.[26] In Fig. 4 (a), i.e., YU300, the length of the directors and the reflector are 130 nm and 300 nm, respectively. At the emission wavelength of the nanowire, $\lambda = 870$ nm (vertical dashed line), both rods are off-resonance. The resonance frequency for the 130 nm rod is at a shorter wavelength, while it is at a longer wavelength for the 300 nm rod. However, the scattering efficiency is similar for both rods at 870 nm. In YU175, (Fig. 4 (b)), the longer rod, i.e., the reflector, is at resonance at $\lambda = 870$ nm by setting its length to 175 nm, . Consequently, the scattering efficiency for this element is $\sim$7 times larger than for the shorter rods, i.e., the directors.

The scattering efficiency simulations have been fitted to Lorentzian functions (red dotted curves in Fig. (a) and (b)) describing the harmonic charge oscillation of the surface plasmons in order to estimate the phase difference between the induced polarization vector and the incident electric field. In Figs. 4 (c) and (d), the Lorentz oscillator phase is represented for the rods of YU300 and YU175, respectively. In YU300, (Fig. 4 (c)), at $\lambda = 870$ nm, the charge oscillation in the rods with the length of 130 nm (director) and 300 nm (reflector)

are approximately in anti-phase with respect to each other; while, for YU175 (Fig. 4 (d)) the relative phase difference between director and reflectors is much smaller.

In YU175, the amplitude of the scattered field by the rods leads to strong scattering by the reflector and relatively weak scattering by the directors. This difference in scattering efficiency, together with the relative phase of the scattered field by the reflector and the directors, prevents the scattered field from the reflector element to destructively interfere with the emission of the nanowire along the backward direction. However, when the length of the reflector element is 300 nm, the resonance frequency is significantly red shifted with respect to the emission peak of nanowire at $\lambda = 870$ nm. Hence, the scattering efficiencies of the reflector and directors are similar at the nanowire emission wavelength. This condition, together with the anti-phase oscillation of the localized surface plasmons, leads to the effective cancellation of the emission from the nanowire in the backward direction.

The spectral difference between the resonance peaks in Fig. 4 (a) and (b), for the reflectors and directors shows a flexible range of operational wavelengths for the emitting element. Since the emission peak of the GaAs nanowire is centered at $\lambda = 870$ nm, we do not have the possibility of varying this wavelength. However, changing GaAs to other materials will still lead to significant directionality as long as the emission is in the range where the scattering efficiencies of reflector and directors are similar.

The full 3D simulation of the antenna emission and the electric field components originating from an electric dipole embedded in the nanowire can provide deeper insight regarding the performance of the antennas. Figures 4 (e) and (f) show snap-shots of the near field amplitude in the xy plane of the E_y electric field component. This is the dominant field component of the emission for YU300 and YU175, respectively. The first conspicuous feature related to the performance of the antennas is the phase difference between reflector and the directors that can be appreciated qualitatively by the color coded E_y. The temporal evolution of the electric field shows that in one period of oscillation of the radiating dipole in YU175 the phase difference between the reflector and first director is similar as described

earlier. This does not provide the proper interference condition for beaming in the forward direction. On the contrary, for YU300, the phase difference between these two elements provides a destructive interference on the backward direction and beaming in forward direction. An animation of scattered near-fields for the two different designs is provided in the supplementary information.

In conclusion, we have demonstrated strong directional emission of GaAs nanowires by coupling this emission to a Yagi-Uda nanoantenna fabricated around the nanowire. This structure forms a hybrid metallic-semiconductor optical antenna. We have also demonstrated that the directionality of the emission can be modified by varying the size of the elements forming the antenna. FDTD simulations of the emission shows excellent agreement with the experimental data. The mechanism leading to this directionality is explained by calculation of scattering efficiencies of the individual metallic elements of the antenna and by full electrodynamic 3D simulations of the full structures. These results constitute the first steps toward the realization of electrically driven directional antennas based on semiconductor nanowires.

Methods

Fabrication

We have used thin (diameter$<$ 100 nm) nanowires to minimize the coupling of the emission to guided modes supported by the nanowire.[17] Due to the recent advancement of the semiconductor growth technology, GaAs nanowires with high degree of control on the geometry and the doping concentration can be achieved.[38] The GaAs nanowires were grown on Si(111) undoped wafer via Ga-assisted method in DCA P600 solid source MBE machine. A Ga rate of 0.3 Å/s as flux of 2.5×10^{-6} torr and a substrate temperature of 640 °C was used for the growth process. During growth, the substrate was rotated by 7 r.p.m. and a V/III beam equivalent pressure ratio of 50. Applying these conditions give rise to the growth of

nanowires with a diameter of 55 nm and length of approximately 12 μm. After the growth of the nanowire core, a 4 nm layer of $Al_xGa_{1-x}As$ (x=0.3) and another 3 nm capping layer of GaAs were grown by changing the growth conditions to the '*two-dimensional epitaxy*'.[39] The presence of $Al_xGa_{1-x}As$ layer passivates the core of the nanowire and decreases the destructive non-radiative surface recombination.[40–43] At the end of the process, the final diameter of the nanowire is $\sim$ 70 nm. The nanowires were removed from the as grown silicon substrate in an isopropanol solution by ultrasonic bath for 1 minute.A few drops of the isopropanol solution containing nanowires were transferred to a patterned fused silica substrate. After the dispersion of the nanowires on the substrate, the position of the nanowires was recognized with optical microscopy. Each area on the pattered substrate encoded the relative position of the nanowire on the wafer. The nanoantennas around the individual nanowires were designed by custom-made software and translated to the files to write e-beam structures. The final position of the nanowires was assigned by a '*shape recognition algorithm*' giving rise to position accuracy of less than 50 nm.[44] The substrate was spin coated by a double resist layer of MMA and PMMA and 10 nm of Cr was evaporated on top of the resist in order to discharge the charge accumulation during e-beam lithography. After the lithography step, Cr was etched and the evaporation of 5nm Ti and 50 nm Au was performed. The presence of Ti improves the adhesion of gold to the silica substrate.

Table 1 shows the geometrical dimensions of the antenna elements measured by SEM. The details of the fabrication are described in the methods section of the article. It should be noted that all the measurements on bare nanowire, YU175 and YU300 are done on separate nanowires taken from the same growth batch. nanowire, L_r and L_d are the lengths of the reflector and directors, respectively, w is the width of the metallic rods, a_r is the distance between the center of the reflector to the center of the nanowire and a_d is the distance between the center of the director to the center of the nanowire and the distance between the directors.

Table 1: The dimensions of the fabricated Yagi Uda + nanowire hybrid antennas. All the dimensions are in nm.

Antenna	d_{nw}	L_r	L_d	w	a_r	a_d	L_{total}
YU175	75	175	130	60	185	205	860
YU300	75	300	130	60	155	120	575

Numerical simulations

The simulations of the radiation patterns were performed with the Finite-Difference Time-Domain method (Lumerical's FDTD Solution). The GaAs nanowire with the length of 6 μm and the diameter of 70 nm is placed horizontally on top of a silica substrate. The medium on top of the substrate is considered to be air (n=1). The optical constants of GaAs were taken from Palik.[45] An oscillating electrical dipole along the long axis of the nanowire is considered as the emission source. The near-field components of the electric field were detected by a planar monitor parallel to the substrate. The far-field patterns were calculated using the near-field to far-field conversion method.

Acknowledgement

We thank Sander Mann for the careful checking of the manuscript. This work has been implemented under the support of Schweizerischer Nationalfonds (SNF) through project number 137648 and 156081, European Union's Initial Training Networks (ITN), Netherlands Foundation for Fundamental Research on Matter (FOM) and the Netherlands Organization for Scientific Research (NWO), and is part of an industrial partnership program between Philips and FOM.

Supporting Information Available

Supporting information shows the schematic representation of the Fourier setup, dispersion of the leaky and guided modes in GaAs nanowires, absorption and scattering efficiencies of

the antenna elements , effect of the number of directors on the directionality, near field map of intensity enhancement and animations of the y-component of scattered near-fields for two different antennas.

This material is available free of charge via the Internet at `http://pubs.acs.org/`.

References

(1) Li, Y.; Qian, F.; Xiang, J.; Lieber, C. M. Nanowire electronic and optoelectronic devices. *Materials Today* **2006**, *9*, 18 – 27.

(2) Yan, R.; Gargas, D.; Yang, P. Nanowire photonics. *Nat Photon* **2009**, *3*, 569–576.

(3) Yang, P.; Yan, R.; Fardy, M. Semiconductor Nanowire: What's Next? *Nano Letters* **2010**, *10*, 1529–1536, PMID: 20394412.

(4) Thelander, C.; Agarwal, P.; Brongersma, S.; Eymery, J.; Feiner, L.; Forchel, A.; Scheffler, M.; Riess, W.; Ohlsson, B.; Gösele, U.; Samuelson, L. Nanowire-based one-dimensional electronics. *Materials Today* **2006**, *9*, 28 – 35.

(5) Saxena, D.; Mokkapati, S.; Parkinson, P.; Jiang, N.; Gao, Q.; Tan, H. H.; Jagadish, C. Optically pumped room-temperature GaAs nanowire lasers. *Nat Photon* **2013**, *7*, 963–968.

(6) Duan, X.; Huang, Y.; Agarwal, R.; Lieber, C. M. Single-nanowire electrically driven lasers. *Nature* **2003**, *421*, 241–245.

(7) Kelzenberg, M. D.; Boettcher, S. W.; Petykiewicz, J. A.; Turner-Evans, D. B.; Putnam, M. C.; Warren, E. L.; Spurgeon, J. M.; Briggs, R. M.; Lewis, N. S.; Atwater, H. A. Enhanced absorption and carrier collection in Si wire arrays for photovoltaic applications. *Nat Mater* **2010**, *9*, 239–244.

(8) Krogstrup, P.; Jorgensen, H. I.; Heiss, M.; Demichel, O.; Holm, J. V.; Aagesen, M.; Nygard, J.; Fontcuberta i Morral, A. Single-nanowire solar cells beyond the Shockley-Queisser limit. *Nat Photon* **2013**, *7*, 306–310.

(9) Wallentin, J.; Anttu, N.; Asoli, D.; Huffman, M.; Åberg, I.; Magnusson, M. H.; Siefer, G.; Fuss-Kailuweit, P.; Dimroth, F.; Witzigmann, B.; Xu, H. Q.; Samuelson, L.; Deppert, K.; Borgström, M. T. InP Nanowire Array Solar Cells Achieving 13.8Ray Optics Limit. *Science* **2013**, *339*, 1057–1060.

(10) Piccione, B.; Cho, C.-H.; van Vugt, L. K.; Agarwal, R. All-optical active switching in individual semiconductor nanowires. *Nat Nano* **2012**, *7*, 640–645.

(11) Claudon, J.; Bleuse, J.; Malik, N. S.; Bazin, M.; Jaffrennou, P.; Gregersen, N.; Sauvan, C.; Lalanne, P.; Gerard, J.-M. A highly efficient single-photon source based on a quantum dot in a photonic nanowire. *Nat Photon* **2010**, *4*, 174–177.

(12) Bulgarini, G.; Reimer, M. E.; Bouwes Bavinck, M.; Jöns, K. D.; Dalacu, D.; Poole, P. J.; Bakkers, E. P. A.; Zwiller, V. Nanowire Waveguides Launching Single Photons in a Gaussian Mode for Ideal Fiber Coupling. *Nano Letters* **2014**, *14*, 4102–4106.

(13) Maslov, A. V.; Ning, C. Z. Far-field emission of a semiconductor nanowire laser. *Opt. Lett.* **2004**, *29*, 572–574.

(14) Maslov, A. V.; Bakunov, M. I.; Ning, C. Z. Distribution of optical emission between guided modes and free space in a semiconductor nanowire. *Journal of Applied Physics* **2006**, *99*, –.

(15) Cao, L.; White, J. S.; Park, J.-S.; Schuller, J. A.; Clemens, B. M.; Brongersma, M. L. Engineering light absorption in semiconductor nanowire devices. *Nat Mater* **2009**, *8*, 643–647.

(16) Grzela, G.; Paniagua-Domínguez, R.; Barten, T.; Fontana, Y.; Sánchez-Gil, J. A.; Gómez Rivas, J. Nanowire Antenna Emission. *Nano Letters* **2012**, *12*, 5481–5486.

(17) Paniagua-Dominguez, R.; Grzela, G.; Rivas, J. G.; Sanchez-Gil, J. A. Enhanced and directional emission of semiconductor nanowires tailored through leaky/guided modes. *Nanoscale* **2013**, *5*, 10582–10590.

(18) Muskens, O. L.; Treffers, J.; Forcales, M.; Borgström, M. T.; Bakkers, E. P. A. M.; Rivas, J. G. Modification of the photoluminescence anisotropy of semiconductor nanowires by coupling to surface plasmon polaritons. *Opt. Lett.* **2007**, *32*, 2097–2099.

(19) Brittman, S.; Gao, H.; Garnett, E. C.; Yang, P. Absorption of Light in a Single-Nanowire Silicon Solar Cell Decorated with an Octahedral Silver Nanocrystal. *Nano Letters* **2011**, *11*, 5189–5195, PMID: 22082022.

(20) Casadei, A.; Pecora, E. F.; Trevino, J.; Forestiere, C.; Rüffer, D.; Russo-Averchi, E.; Matteini, F.; Tutuncuoglu, G.; Heiss, M.; Fontcuberta i Morral, A.; Dal Negro, L. Photonic–Plasmonic Coupling of GaAs Single Nanowires to Optical Nanoantennas. *Nano Letters* **2014**, *14*, 2271–2278.

(21) Anger, P.; Bharadwaj, P.; Novotny, L. Enhancement and Quenching of Single-Molecule Fluorescence. *Phys. Rev. Lett.* **2006**, *96*, 113002.

(22) Kühn, S.; Håkanson, U.; Rogobete, L.; Sandoghdar, V. Enhancement of Single-Molecule Fluorescence Using a Gold Nanoparticle as an Optical Nanoantenna. *Phys. Rev. Lett.* **2006**, *97*, 017402.

(23) Muskens, O. L.; Giannini, V.; Sánchez-Gil, J. A.; Gómez Rivas, J. Strong Enhancement of the Radiative Decay Rate of Emitters by Single Plasmonic Nanoantennas. *Nano Letters* **2007**, *7*, 2871–2875.

(24) Curto, A. G.; Volpe, G.; Taminiau, T. H.; Kreuzer, M. P.; Quidant, R.; van Hulst, N. F. Unidirectional Emission of a Quantum Dot Coupled to a Nanoantenna. *Science* **2010**, *329*, 930–933.

(25) Novotny, L.; van Hulst, N. Antennas for light. *Nat Photon* **2011**, *5*, 83–90.

(26) Li, J.; Salandrino, A.; Engheta, N. Shaping light beams in the nanometer scale: A Yagi-Uda nanoantenna in the optical domain. *Phys. Rev. B* **2007**, *76*, 245403.

(27) Hofmann, H. F.; Kosako, T.; Kadoya, Y. Design parameters for a nano-optical Yagi–Uda antenna. *New Journal of Physics* **2007**, *9*, 217.

(28) Koenderink, A. F. Plasmon Nanoparticle Array Waveguides for Single Photon and Single Plasmon Sources. *Nano Letters* **2009**, *9*, 4228–4233, PMID: 19835368.

(29) Kosako, T.; Kadoya, Y.; Hofmann, H. F. Directional control of light by a nano-optical Yagi-Uda antenna. *Nat Photon* **2010**, *4*, 312–315.

(30) Coenen, T.; Vesseur, E. J. R.; Polman, A.; Koenderink, A. F. Directional Emission from Plasmonic Yagi–Uda Antennas Probed by Angle-Resolved Cathodoluminescence Spectroscopy. *Nano Letters* **2011**, *11*, 3779–3784, PMID: 21780758.

(31) Dorfmüller, J.; Dregely, D.; Esslinger, M.; Khunsin, W.; Vogelgesang, R.; Kern, K.; Giessen, H. Near-Field Dynamics of Optical Yagi-Uda Nanoantennas. *Nano Letters* **2011**, *11*, 2819–2824.

(32) Novotny, L.; Hecht, B. *Principles of Nano-Optics*, second edition ed.; Cambridge University Press, 2012.

(33) Fontana, Y.; Grzela, G.; Bakkers, E.; Rivas, J. Mapping the directional emission of quasi-two-dimensional photonic crystals of semiconductor nanowires using Fourier microscopy. *Phys. Rev. B* **2012**, *86*, 245303.

(34) Stratton, J. A. *Electromagnetic Theory. Interntional Series in Pure and Applied Physics*; McGraw-Hill Book Company, 1941.

(35) Wang, J.; Gudiksen, M. S.; Duan, X.; Cui, Y.; Lieber, C. M. Highly Polarized Photoluminescence and Photodetection from Single Indium Phosphide Nanowires. *Science* **2001**, *293*, 1455–1457.

(36) Rümke, T. M.; Sánchez-Gil, J. A.; Muskens, O. L.; Borgström, M. T.; Bakkers, E. P.; Rivas, J. G. Local and anisotropic excitation of surface plasmon polaritons by semiconductor nanowires. *Opt. Express* **2008**, *16*, 5013–5021.

(37) Bolinsson, J.; Mergenthaler, K.; Samuelson, L.; Gustafsson, A. Diffusion length measurements in axial and radial heterostructured nanowires using cathodoluminescence. *Journal of Crystal Growth* **2011**, *315*, 138 – 142, 15th International Conference on Metalorganic Vapor Phase Epitaxy (ICMOVPE-XV).

(38) Dufouleur, J.; Colombo, C.; Garma, T.; Ketterer, B.; Uccelli, E.; Nicotra, M.; Fontcuberta i Morral, A. P-Doping Mechanisms in Catalyst-Free Gallium Arsenide Nanowires. *Nano Letters* **2010**, *10*, 1734–1740.

(39) Heigoldt, M.; Arbiol, J.; Spirkoska, D.; Rebled, J. M.; Conesa-Boj, S.; Abstreiter, G.; Peiro, F.; Morante, J. R.; Fontcuberta i Morral, A. Long range epitaxial growth of prismatic heterostructures on the facets of catalyst-free GaAs nanowires. *J. Mater. Chem.* **2009**, *19*, 840–848.

(40) Titova, L. V.; Hoang, T. B.; Jackson, H. E.; Smith, L. M.; Yarrison-Rice, J. M.; Kim, Y.; Joyce, H. J.; Tan, H. H.; Jagadish, C. Temperature dependence of photoluminescence from single core-shell GaAs–AlGaAs nanowires. *Applied Physics Letters* **2006**, *89*.

(41) Demichel, O.; Heiss, M.; Bleuse, J.; Mariette, H.; Fontcuberta i Morral, A. Impact of surfaces on the optical properties of GaAs nanowires. *Applied Physics Letters* **2010**, *97*.

(42) Casadei, A.; Schwender, J.; Russo-Averchi, E.; Rüffer, D.; Heiss, M.; Alarcó-Lladó, E.; Jabeen, F.; Ramezani, M.; Nielsch, K.; Morral, A. F. i. Electrical transport in C-doped GaAs nanowires: surface effects. *physica status solidi (RRL) – Rapid Research Letters* **2013**, *7*, 890–893.

(43) Joyce, H. J.; Docherty, C. J.; Gao, Q.; Tan, H. H.; Jagadish, C.; Lloyd-Hughes, J.; Herz, L. M.; Johnston, M. B. Electronic properties of GaAs, InAs and InP nanowires studied by terahertz spectroscopy. *Nanotechnology* **2013**, *24*, 214006.

(44) `http://www.qstarter.ch/projects/automated-contacting-of-random-microstructures`, accessed Jan 2014.

(45) Palik, E. D. *Handbook of Optical Constants of Solids*; Academic Press, 1998.

Graphical TOC Entry